LA-UR-01-4540
Approved for public release; distribution is unlimited.

Title:

IMAGING MAGNETIC SOURCES IN THE PRESENCE OF SUPERCONDUCTING SURFACES: MODEL & EXPERIMENT

Author(s): Volegov, P., Kraus, Jr., R.H., Maharajh, K., Matlachov, A., Espy, M., and E.R.Flynn

Submitted to:

IMAGING MAGNETIC SOURCES IN THE PRESENCE OF SUPERCONDUCTING SURFACES: MODEL & EXPERIMENT

Volegov, P., Kraus, Jr., R.H., Maharajh, K., Matlachov, A., Espy, M., and E.R.Flynn

Los Alamos National Laboratory, Los Alamos, NM USA
University of New Mexico, Albuquerque, NM, USA

Introduction

The forward physics model describing the effect of a superconducting surface on the magnetic field distribution resulting from specific magnetic sources has numerous applications ranging from basic physics experiments to large superconducting magnets used in energy storage and magnetic resonance imaging. In this paper, we describe the novel application of a superconducting imaging surface (SIS) to enhance the performance of systems designed to directly observe and localize human brain function. Magnetoencephalography (MEG) measures the weak magnetic fields emanating from the brain as a direct consequence of the neuronal currents resulting from brain function[1]. The extraordinarily weak magnetic fields are measured by an array of SQUID (Superconducting QUantum Interference Device) sensors. The position and vector characteristics of these neuronal sources can be estimated from the inverse solution of the field distribution at the surface of the head. In addition, MEG temporal resolution is unsurpassed by any other method currently used for brain imaging. Although MEG source reconstruction is limited by solutions of the electromagnetic inverse problem, constraints used for source localization produce reliable results.

A novel MEG system incorporating a SIS has been designed and built at Los Alamos with the goal of dramatically improving source localization accuracy while mitigating limitations of current systems (e.g. low signal-to-noise, cost, bulk). We incorporate shielding and source field measurement into an integrated design and combine the latest SQUID and data acquisition technology. The Los Alamos MEG system is based on the principal that fields from nearby sources measured by a SQUID sensor array while the SIS simultaneously shields the sensor array from distant noise fields. In general, Meissner currents flow in the surface of superconductors, preventing any significant penetration of magnetic fields. A hemispherical SIS with a brim, or helmet, surrounds the SQUID sensor array largely sheilding the SQUID sensors from sources outside the helmet.

We present the general derivation of the forward model used to describe the effect of a SIS on source fields. Experimental data for the SIS-MEG system are compared with computed field distributions for a comprehensive set of sources.

Method

Localizing sources of neuronal activation from MEG measurements requires a complete description of the "forward physics" that describes how neuronal currents lead to magnetic fields at the SQUID sensors. The forward model required for MEG must include the complex neuronal source model that incorporates intracellular ionic currents, intercellular and extracellular volume currents, brain structure, and conductivities. The forward model for our SIS-MEG system must further include the effect of the superconducting surface on the fields generated by all of the primary sources. We have separated the problem into the forward description of the source and the effect of the SIS on the source fields, and assume the effect of field perturbations cause by the SIS on the primary source is negligible. We derive here the forward physics and a numerical model for computing the forward fields assuming a known source model.

An analytic description of the fields at the sensors requires that the homogenous solution corresponding to the free space fields are added to any source(s) and include the superconductor boundary condition. Solutions are known for simple geometries such as the sphere or infinite plane [2], but for finite geometries the field will be very difficult if not impossible to determine analytically. Therefore we have developed a numeric procedure to calculate the magnetic field in the presence of *any* arbitrarily shaped superconducting surface.

Conceptually our model computes a net surface magnetization resulting from the Meissner currents[3] for which the normal component of the magnetic field equals the negative free space magnetic field normal component at the surface, e.g. $\boldsymbol{B}_{\perp}(\text{surface}) = 0$, the boundary condition at superconducting surfaces. In practice, we have chosen to use a finite element method (FEM) to numerically solve the problem. The superconducting surface is divided into a mesh of triangular elements, each of which is assigned a uniform magnetization. Conceptually, the magnetization in each triangular element results from a distribution of currents in that element as described by Meissner. A current flowing along the edge of each triangular element is used to describe the magnetic field. The net magnetic field at each triangular surface element is a superposition of the primary field and the fields produced by all triangular elements. Using the Biot-Savart law to describe the field from each segment of the triangle and summing over the three edges results in:

$$\mathbf{B}_{net}(\mathbf{r}) = \mathbf{B}_p(\mathbf{r}) + \frac{\mu_0}{4\pi}\sum_{j=1}^{m} I_j *$$
$$\left(\sum_{i=0}^{2}[\mathbf{r}_j^{(i)} \times \mathbf{r}_j^{(i+1)}]\frac{(r_j^{(i)} + r_j^{(i+1)})}{r_j^{(i)} r_j^{(i+1)}(r_j^{(i)} r_j^{(i+1)} + (\mathbf{r}_j^{(i)} \cdot \mathbf{r}_j^{(i+1)}))}\right)$$
$$\mathbf{r}_j^{(i)} = \mathbf{r} - \mathbf{v}_j^{(i \bmod 3)}$$

where $\mathbf{r}_j$ are the positions from the endpoints to the observer, $v_j^{(0,1,2)}$ are vertices of the j^{th} cell, I_j is equivalent magnetization current for that cell, and $\mathbf{B}_p$ is primary (free space) magnetic field resulting from a current density, $\mathbf{J}$. The boundary condition requires the normal component of the net magnetic field to vanish at the superconducting surface, and using collocation method we can write m linear equations for I_j:

$$\sum_{j=1}^{m} A_{ij} I_j = -b_i, \quad i = \overline{1,m}$$
$$A_{ij} = \frac{\mu_0}{4\pi} \cdot \mathbf{n}_i \cdot$$
$$\left(\sum_{k=0}^{2}[\mathbf{r}_{ij}^{(k)} \times \mathbf{r}_{ij}^{(k+1)}]\frac{(r_{ij}^{(k)} + r_{ij}^{(k+1)})}{r_{ij}^{(k)} r_{ij}^{(k+1)}(r_{ij}^{(k)} r_{ij}^{(k+1)} + (\mathbf{r}_{ij}^{(k)} \cdot \mathbf{r}_{ij}^{(k+1)}))}\right)$$
$$b_i = \mathbf{n}_i \cdot \mathbf{B}_p(\mathbf{p}_i), \quad \mathbf{r}_{ij}^{(k)} = \mathbf{p}_i - \mathbf{v}_j^{(k \bmod 3)}$$

where $\{\mathbf{p}_i\}_1^m$ are m points at the center of each i^{th} cell on the superconducting surface, and $\mathbf{n}_i$ is the unit vector normal to the surface at the i^{th} cell. In summary, our forward model describes the superconducting surface as a triangular finite element mesh and the free space field for the primary source(s) is calculated at each mesh element. The magnetization for all elements are calculated according to the above equations.

Results

THE FEM model was tested using a novel SIS-MEG system designed and built by the Biophysics Group at the Los Alamos National Laboratory. This system incorporates a complicated helmet-shaped SIS that surrounds an array of 150 SQUID sensors. We have constructed a precision multi-source phantom to generate well-characterized source fields that will severely test the FEM approach to calculating the effect of the SIS on those fields, both inside and outside the SIS helmet.

The SIS is fabricated from lead (Type I superconductor below ~7 Kelvins) with a complex shape consisting of a 5.064inch radius hemisphere with two small "cut-outs" at opposite sides of the hemisphere, and a 2-inch brim that is smoothly melded to the edge of the modified hemisphere. An array of 150 SQUID magnetometers is mounted on "studs" at offsets from the SIS ranging from 1cm to 3cm. The SQUID-SIS offsets were allowed to vary in order to place each sensor as close to the head-shaped dewar surface, and consequently the subject head, as possible. The entire system is operated in a liquid helium bath at ~4 Kelvins temperature. Magnetic fields produced by sources inside the helmet (e.g. from a subject brain or a 'calibration phantom') are detected by the SQUID magnetometers. Various sets of fixed magnetic dipole coils known as a 'phantoms' (that emulate signals produced by the human brain) have been constructed to measure the effects of the SIS in the Los Alamos MEG system and quantify overall system performance. Simple dry-wire phantoms, for which the source model can be completely described, were used to eliminate any source model dependence from our results. Three orthogonal coils were located at most positions to study correlations between localization accuracy and source orientation. Each phantom coil was precisely machined and located relative to the phantom 'origin' with absolute precision better than 25µm and 10mRad. While the relative position and orientation of each phantom coil is precisely known, the *a priori* position of the phantom relative to the SQUID array is known to ~±1cm. Although the SQUID array was fabricated to better than ±50µm overall tolerance, cooling from ~300K to 4K causes significant symmetric and asymmetric contractions; consequently we assumed initial ±1mm and ±100mRad sensor position and orientation accuracy. SQUID sensitivities were calibrated prior to installation into the MEG system to a precision of 0.5%, however a systematic error discovered later may increase the total error to as much as 1%.

The FEM mesh used to describe the SIS for the whole-head MEG system in the numerical model was derived from the exact "as built" geometry of the lead helmet. All aspects of the SIS including the hemispherical core, cut-outs for the ears, and brim were represented by the mesh. A 2734 element mesh was generated with approximately equal mesh size over the entire geometry. Once the mesh is generated and the source locations are specified, the numerical forward model is used to calculate the magnetic fields at the sensors positions for each source specified.

Data were acquired for all 150 SQUID sensors while each phantom coils was excited individually by a current-regulated signal generator at 77Hz. Data were acquired by simultaneously sampling 24-bit Delta-Sigma digitizers at 3 kSa/sec at each of the 150 sensor locations. The digitizers were run with high-pass filters disabled and low-pass anti-aliasing filters at 1.2kHz. The raw data were digitally filtered using a band-pass algorithm that produced minimal artifacts was implemented in MATLAB and signal amplitudes for each spectra were determined using standard FFT techniques.

A representative sample of the calculated and measured fields for the phantom coils is shown in Figure 1 where the fields for two sets of coils are illustrated for a location near the apex of the SIS and one location near the periphery. Each set of coils consisted of one producing a magnetic dipole field oriented approximately radial to the SIS and two producing dipole fields roughly tangential to the SIS and orthogonal to one another. The field patterns are clearly evident in the figure. Inspection of Figure 1 shows extremely good agreement between model and experimental field distributions.

Differences between measured and computed fields were less than 1% for all sensors for which any signifi-

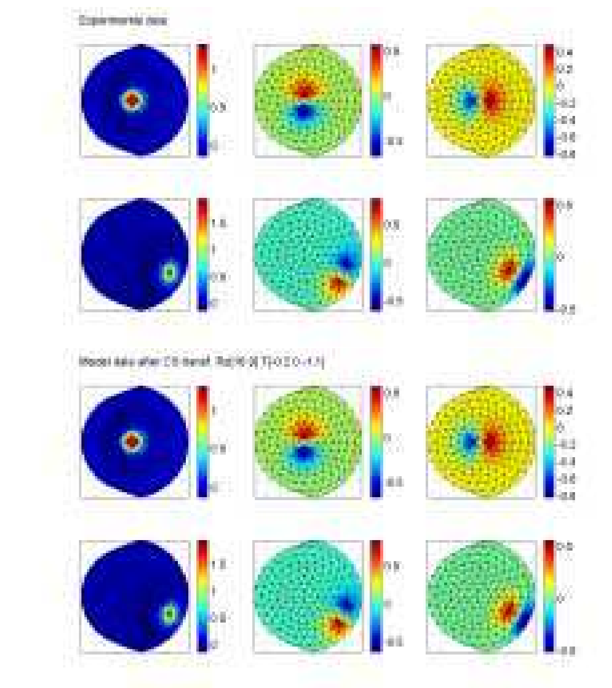

Figure 1: Comparison of magnetic field distributions for six representative phantom sources near the apex and edge of the SIS helmet. **1a:** (left) Measured results, and **1b:** (right) FEM model results

cant field was measured, typically significantly less than 1%. The difference between experimental and model data is presented in the Figure 2. We anticipate that the difference between the measured and computed results will be significantly reduced once a careful analysis of sensor location and orientation is completed and a more dense mesh is used in the calculation.

Conclusion

In conclusion, results computed using our FEM approach agree extremely well with theoretical results for spherical and infinite plane SIS geometries where simple analytic solutions can be derived. Differences between the FEM and analytic results were traced to edge effects and errors caused by finite mesh size and extent. An analytic solution for the more complicated geometry of the SIS 'helmet' used in the Los Alamos MEG system could not be derived; consequently we compared FEM results to experimentally measured field distributions of a wide variety of sources. Measured results agreed extremely well with those computed by our FEM model. Discrepancy between the measured and computed results, though small, can readily be attributed to errors in SQUID magnetometer location and orientation and in finite mesh size effects. In addition, precise calibration of phantom source strength had not been performed prior to the experimental measurements. We have found that a FEM approach provides a powerful and robust method for describing the effect of an arbitrarily shaped SIS on magnetic field distributions.

The ultimate goal of the SIS-MEG system is to precisely localize sources within a human brain. A detailed under-

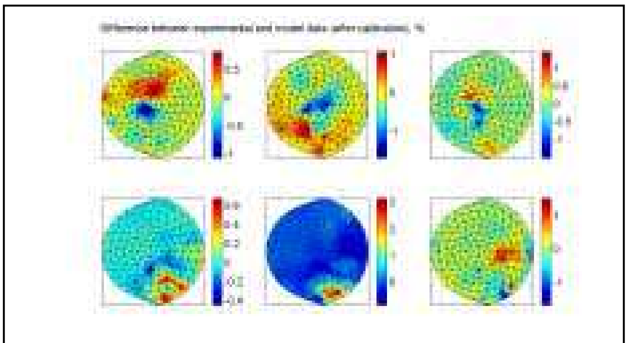

Figure 2: Difference between measured and FEM model data, normalized to coil signal maxima.

standing of how various measurement and modeling errors impact source localization must be obtained in order to determine the degree to which the sources of these errors must be controlled. We are currently implementing an algorithm to solve the inverse problem of electromagnetism for both localizing magnetic field sources using a set of field measurements and localizing a sensor using a set of magnetic field distributions. Using data from a set of precision magnetic field sources, we will calibrate the position and orientation of each SQUID sensor, and anticipate a dramatic reduction in field error. The FEM description of the SIS helmet used in the Los Alamos MEG system will become an integral part of the forward physics description of the system. ed.

References

[1] Hämäläinen, M., Hari, R., Ilmoniemi, R. J., Knuutila, J., and Lounasmaa, O. V., Rev. Mod. Physics **65**, 413-497 (1993)

[2] van Hulsteyn, D.B., Petschek, A.G., Flynn, E. R., and Overton, W.C., Rev. Sci. Instr. 66, 3777-3784. 1995

[3] Meissner, W., Naturwissenschaften, **21**, 787 (1933).

Acknowledgements

We gratefully acknowledge the support of the US National Institutes of Health (NINDS), US Department of Energy (OBER) and the National Foundation for Functional Brain Imaging.